J Physiol 587.14 (2009) pp 3587–3603

The Journal of Physiology

Nitric oxide-induced biphasic mechanism of vascular relaxation via dephosphorylation of CPI-17 and MYPT1

Toshio Kitazawa[1], Shingo Semba[1], Yang Hoon Huh[1], Kazuyo Kitazawa[1] and Masumi Eto[2]

[1] *Boston Biomedical Research Institute, 64 Grove Street, Watertown, MA, USA*
[2] *Department of Molecular Physiology and Biophysics, Thomas Jefferson University, 1020 Locust Street, Philadelphia, PA 19107, USA*

Nitric oxide (NO) from endothelium is a major mediator of vasodilatation through cGMP/PKG signals that lead to a decrease in Ca^{2+} concentration. In addition, NO-mediated signals trigger an increase in myosin light chain phosphatase (MLCP) activity. To evaluate the mechanism of NO-induced relaxation through MLCP deinhibition, we compared time-dependent changes in Ca^{2+}, myosin light chain (MLC) phosphorylation and contraction to changes in phosphorylation levels of CPI-17 at Thr38, RhoA at Ser188, and MYPT1 at Ser695, Thr696 and Thr853 in response to sodium nitroprusside (SNP)-induced relaxation in denuded rabbit femoral artery. During phenylephrine (PE)-induced contraction, SNP reduced CPI-17 phosphorylation to a minimal value within 15 s, in parallel with decreases in Ca^{2+} and MLC phosphorylation, followed by a reduction of contractile force having a latency period of about 15 s. MYPT1 phosphorylation at Ser695, the PKG-target site, increased concurrently with relaxation. Phosphorylation of RhoA, MYPT1 Thr696 and Thr853 differed significantly at 5 min but not within 1 min of SNP exposure. Inhibition of Ca^{2+} release delayed SNP-induced relaxation while inhibition of Ca^{2+} channel, BK_{Ca} channel or phosphodiesterase-5 did not. Pretreatment of resting artery with SNP suppressed an increase in Ca^{2+}, contractile force and phosphorylation of MLC, CPI-17, MYPT1 Thr696 and Thr853 at 10 s after PE stimulation, but had no effect on phorbol ester-induced CPI-17 phosphorylation. Together, these results suggest that NO production suppresses Ca^{2+} release, which causes an inactivation of PKC and rapid CPI-17 dephosphorylation as well as MLCK inactivation, resulting in rapid MLC dephosphorylation and relaxation.

(Received 10 March 2009; accepted after revision 17 May 2009; first published online 18 May 2009)

Corresponding author T. Kitazawa: Boston Biomedical Research Institute, 64 Grove Street, Watertown, MA 02472, USA. Email: Kitazawa@bbri.org

Abbreviations ACh, acetylcholine; BK_{Ca} channel, large-conductance Ca^{2+}-activated potassium channel; 8Br-cGMP, 8-bromo-guanosine 3′,5′-cyclic monophosphate; CPI-17, protein kinase C-potentiated protein phosphatase inhibitor protein 17 kDa; cPKC, Ca^{2+}-dependent PKC; DAG, diacylglycerol; DN, denuded; ET, endothelium; GPCR, G protein-coupled receptor; IP_3, inositol 1,4,5-trisphosphate; IRAG, IP_3 receptor-associated PKG substrate; L-NAME, L-N^G-nitroarginine methyl ester; MBCQ, 4-[[3,4-(methylenedioxy)benzyl]amino]-6-chloroquinazoline; MLCK, Ca^{2+}–calmodulin-dependent myosin light chain kinase; MLC, myosin light chain; MLCP, myosin light chain phosphatase; MYPT1, myosin targeting subunit of MLCP; NO, nitric oxide; PAGE, polyacrylamide gel electrophoresis; PDBu, phorbol 12,13-dibutyrate; PDE5, phosphodiesterase 5 isoform; PE, phenylephrine; PKA, cAMP-dependent protein kinase; PKC, protein kinase C; PKG, cyclic GMP-dependent protein kinase; PLCβ, phospholipase Cβ; RGS2, regulator of G protein signalling 2; RhoA, member A of Rho family of small GTPases; ROCK, Rho-associated kinase; SDS, sodium dodecyl sulfate; SNAP, *S*-nitroso-*N*-acetylpenicillamine; SNP, sodium nitroprusside; SR, sarcoplasmic reticulum; TCA, trichloroacetic acid; TXA_2, thromboxane A_2.

Nitric oxide (NO) is a crucial regulator of vascular tone and blood pressure, and also plays a pivotal role in the pathogenesis of hypertension, atherosclerosis and other vascular diseases (Lincoln *et al.* 2006; Murad, 2006). Gaseous NO produced in the endothelium rapidly passes into the medium of arterial smooth muscle layers to stimulate soluble guanylyl cyclase to convert GTP to cGMP. Cyclic GMP activates type 1 cGMP-dependent protein kinase (PKG-1), which is a major mediator of NO-induced relaxation as evidenced by the hypertensive phenotype displayed by mice having a conventional or conditional deletion of the PKG-1 gene (Feil *et al.* 2003). In addition, mutations in the N-terminal leucine-zipper domain of the PKG-1α isoform cause a hypertensive phenotype without renal disorder, suggesting a role for smooth muscle PKG-1 in blood pressure control (Michael

DOI: 10.1113/jphysiol.2009.172189

et al. 2008). Several PKG-targeted phospho-proteins and their respondents were found to interfere with smooth muscle contraction at various signalling pathway steps (Hofmann *et al.* 2006), but the temporal relationship between these phosphorylation signals and NO-induced relaxation remains largely unclear.

Smooth muscle contraction is dually regulated by changes in cytoplasmic Ca^{2+} concentration and Ca^{2+} sensitivity of myosin light chain (MLC) phosphorylation. Excitatory agonists activate both heterotrimeric Gq and $G_{12/13}$ G proteins by binding to their specific G protein-coupled receptor (GPCR) (Somlyo & Somlyo, 2003). Gq activates phospholipase Cβ (PLCβ) to produce two messengers, inositol 1,4,5-trisphosphate (IP_3) and diacylglycerol (DAG). IP_3 induces Ca^{2+} release from the sarcoplasmic reticulum (SR), which triggers a rapid increase in MLC phosphorylation and contraction through activation of classical Ca^{2+}–calmodulin-dependent MLC kinase (MLCK): i.e. Gq/PLCβ/IP_3/Ca^{2+}/MLCK (Taylor & Stull, 1988). The other rapid messenger, DAG, in concert with Ca^{2+}, activates Ca^{2+}-dependent PKC (cPKC) to phosphorylate Thr38 of CPI-17 (Eto *et al.* 1997), a phosphorylation-dependent inhibitor protein of MLC phosphatase (MLCP; Hartshorne *et al.* 2004). Phosphorylated CPI-17 inhibits MLCP activity, which results in an increase in the Ca^{2+} sensitivity of MLC phosphorylation upon Ca^{2+} release from SR: Gq/PLCβ/(Ca^{2+}+DAG)/cPKC/CPI-17/MLCP (Dimopoulos *et al.* 2007). CPI-17-mediated MLCP inhibition with simultaneous MLCK activation (Isotani *et al.* 2004) following agonist-stimulation is responsible for the robust increase in MLC phosphorylation and smooth muscle contraction (Dimopoulos *et al.* 2007).

After the transient Ca^{2+} release from the SR, Ca^{2+} influx occurs mainly through the voltage-dependent L-type Ca^{2+} channel that maintains the tonic level of cytoplasmic Ca^{2+}. Although the Ca^{2+} concentration is lower than that at the initial transient peak in the cytoplasm, it is sufficient to partially activate MLCK (Somlyo & Somlyo, 1994; Isotani *et al.* 2004). In parallel, agonist stimulation of $G_{12/13}$ subsequently activates the small G protein RhoA, which interacts with and activates its downstream target Rho-kinase (ROCK) (Matsui *et al.* 1996; Ishizaki *et al.* 1996; see Fukata *et al.* 2001 for review). Activated ROCK phosphorylates the myosin targeting subunit of MLCP, MYPT1, at Thr853 (in human 133 kDa sequence) but not Thr696 (Kitazawa *et al.* 2003; Niiro *et al.* 2003; Wilson *et al.* 2005; Nakamura *et al.* 2007) as well as CPI-17 at Thr38 (Kitazawa *et al.* 2000) in smooth muscle strips, resulting in MLCP inhibition. RhoA/ROCK-mediated MLCP inhibition, in addition to the partial activation of MLCK via Ca^{2+} influx, may therefore contribute to MLC phosphorylation in the tonic phase of contraction; $G_{12/13}$/RhoA/ROCK/CPI-17 and $G_{12/13}$/RhoA/ROCK/MYPT1(Thr853) (Dimopoulos *et al.* 2007). Thus, two sources of Ca^{2+} from SR and through L-type Ca^{2+} channel account for, respectively, a rapid increase in and maintenance of MLC phosphorylation coupled with the biphasic inhibition of MLCP through a sequential activation of PKC and ROCK.

The NO/cGMP/PKG signalling pathway is known to interfere with either mechanism for agonist-induced increase in cytoplasmic Ca^{2+} or in contractile Ca^{2+} sensitivity (Ca^{2+} sensitization) (Morgan & Morgan, 1984; see Somlyo & Somlyo, 2003 for review). The PKG-1α isoform phosphorylates the regulator of G protein signalling 2 (RGS2) to increase the activity of Gq GTPase (Tang *et al.* 2003) while the PKG-1β isoform phosphorylates the IP_3 receptor-associated PKG substrate (IRAG) to interfere with IP_3-induced Ca^{2+} release via the IP_3 receptor channel (Geiselhöringer *et al.* 2004). Either action results in an inhibition of Gq/PLCβ/IP_3/Ca^{2+}/MLCK and Gq/PLCβ/(Ca^{2+}+DAG)/cPKC/CPI-17/MLCP signalling pathways. The effective lowering of intracellular Ca^{2+} requires not only inhibition of Ca^{2+} release but also Ca^{2+} removal by pumping activity. It has long been proposed that the cGMP/PKG pathway leads to lowering of $[Ca^{2+}]_i$ by activating the SR Ca^{2+}-ATPase (SERCA) (Rashatwar *et al.* 1987; Twort & van Breeman, 1988). The most plausible target site for PKG in this mechanism is phospholamban, a SERCA inhibitory protein that also functions in the cAMP/PKA pathway in cardiac muscle. However, Lalli *et al.* (1999) used a gene targeting approach to demonstrate that relaxation induced by either SNP or forskolin, an adenylate cyclase activator, was not affected by the ablation of phospholamban in aorta smooth muscle. Whether the cGMP-induced activation of Ca^{2+} uptake by the SR results from the direct activation of the Ca^{2+} pump or inhibition of the Ca^{2+} release process is still unclear. PKG-1 also phosphorylates the large-conductance Ca^{2+}-activated K^+ (BK_{Ca}) channel (Alioua *et al.* 1998), causing channel opening followed by membrane hyperpolarization, which inhibits the opening of voltage-dependent Ca^{2+} channel and, as a result, decreases the Ca^{2+} influx to induce a relaxation. In addition, cGMP blocks agonist-induced increase in contractile Ca^{2+} sensitivity (Ca^{2+} sensitization), suggesting reactivation/deinhibition of MLCP (Lee *et al.* 1997; Wu *et al.* 1998) via the following potential mechanisms. PKG-1α-mediated phosphorylation of RhoA at Ser188 inactivates recombinant RhoA (Sauzeau *et al.* 2000). The inactivation of RhoA leads to an inhibition of ROCK, which potentially results in a decrease in ROCK-mediated phosphorylation of MYPT1 Thr853 and CPI-17 Thr38, thus decreasing Ca^{2+} sensitization (Ca^{2+} desensitization). PKG-1-mediated phosphorylation of MYPT1 at Ser695 interferes with phosphorylation of adjacent Thr696 to remove the inhibition of MLCP by

phosphorylated Thr696, reactivate MLCP and decrease Ca^{2+} sensitization (Wooldridge *et al.* 2004; Nakamura *et al.* 2007). In addition, PKG-1α directly interacts with MYPT1 via the N-terminal leucine zipper domain, which is critical for PKG-1α-mediated activation of MLCP (Surks *et al.* 1999; Huang *et al.* 2004), and the blood pressure control (Michael *et al.* 2008). Thus, multiple signals seem to be involved in NO-induced reactivation of MLCP and vasodilatation. Most of these studies have been done using permeabilized smooth muscle and the role of each signal mediated by PKG-1 in NO-induced relaxation is still poorly understood in intact vascular smooth muscle strips, which preserve the biphasic regulation of MLC phosphorylation and contraction in response to agonist stimulation.

We hypothesized that NO interferes with each signalling pathway in the early and late phases that mediate agonist-induced smooth muscle contraction. We therefore examined the temporal relationships among Ca^{2+}, contraction, MLC phosphorylation, phosphorylation of CPI-17 at Thr38, MYPT1 at Ser695, Thr696 and Thr853, and RhoA at Ser188 during sodium nitroprusside (SNP)-induced relaxation in intact rabbit femoral artery. Our results reveal that NO production triggers a biphasic and rapid dephosphorylation of CPI-17 and a slow dephosphorylation of MYPT1 together with inhibition of Ca^{2+} release and influx, respectively, leading to biphasic reactivation of MLCP and inactivation of MLCK.

Methods

Composition of the external solutions

The compositions of external solutions for intact smooth muscle strips were prepared as described previously (Masuo *et al.* 1994). Normal external solution for intact smooth muscle strips was 150 mM NaCl, 4 mM KCl, 2 mM calcium methanesulphonate, 2 mM magnesium methanesulphonate, 5.6 mM glucose, and 5 mM *N*-2-hydroxyethylpiperazine-*N*′-2-ethanesulfonic acid. Depolarizing external solution had 124 mM potassium methanesulphonate substituted equally for NaCl with the other components at the same concentrations. Both solutions were adjusted to pH 7.4 with Tris.

Tissue preparation and force measurement

All animal procedures were approved by the Animal Care and Use Committee of the Boston Biomedical Research Institute. Halothane vapour was used to kill New Zealand White male 2.5–3 kg rabbits. After breathing had completely ceased and any vital signs were stopped, the carotid artery was cut. Femoral arterial smooth muscle strips (~70–80 μm in thickness, 0.75 mm in width and 2.5–3 mm in length) were dissected from 16 rabbits, and the endothelial and connective tissues removed. The denudation of the endothelium layer in the arterial strips was confirmed by their displaying no relaxation in response to 10 μM acetylcholine (ACh) during phenylephrine (PE)-induced contraction. One end of the strip was tied with a silk monofilament between a force transducer (AE801, SensoNor, Horten, Norway) and the other end to a micromanipulator to adjust the muscle length to 1.2–1.3 times slack length, in which the strips produced a maximum force. The strips were mounted in a well on a Bubble chamber plate to allow for either a rapid solution change or quick-freezing by plunging into liquid nitrogen-cooled propane (−150°C) as described previously (Kitazawa *et al.* 1991; Masuo *et al.* 1994). Each strip was repeatedly stimulated for 5 min with 124 mM K^+ solution at intervals of 15 or 20 min until the peak contraction was no longer increased. The strips were then alternately stimulated with high K^+ and 10 μM PE for a few cycles until the PE-induced contraction was no longer increased. The treatment with high K^+ between PE-induced contractions was required to maintain constant SR Ca^{2+} along with a reproducible time course and amplitude of PE-induced contractions.

To deplete Ca^{2+} stores in the SR, the strips were incubated in the normal external solution (see the composition above) containing 1 μM ryanodine (BioMol, Plymouth Meeting, PA, USA) and 20 mM caffeine for 15 min and washed with the same solution without caffeine for another 15 min whereupon caffeine no longer evoked a transient contraction (Kobayashi *et al.* 1989; Dimopoulos *et al.* 2007). The strips were stimulated with PE in the presence of ryanodine.

To block Ca^{2+} influx, the strips were incubated in the normal external solution containing 1 μM nicardipine for 10 min after a 10 min rest and stimulated with PE in the presence of the drug. After treatment, high K^+ did not evoke a significant contraction (Dimopoulos *et al.* 2007).

Sodium nitroprusside (SNP) sensitivity and freezing protocol

SNP-induced relaxation of phenylephrine (PE)-induced contraction. Figure 1*A* illustrates representative time courses for concentration-dependent SNP-induced relaxation of 10 μM PE-induced contraction in denuded rabbit femoral artery smooth muscle strips. The relaxation induced by 10 μM SNP when applied at the peak of contraction 3 min after PE stimulation had a half-time of 28 ± 3 s ($n = 5$) and reached a minimum at about 1 min, which was much shorter than that at 1 μM or less of SNP (Fig. 1*A*) and not significantly different from that seen for 20 μM SNP (not shown). The relaxation had a latent

period of 14 ± 2 s ($n = 11$) at 10–20 μM SNP with longer latency periods accompanying lower SNP concentrations. Figure 1*B* illustrates an average ($n = 5$) time course of 10 μM SNP-induced relaxation with freezing points at 0, 15, 30, 60 and 300 s after SNP addition for measurements of protein phosphorylation during the relaxation. Contractile rebound of SNP-induced relaxation was seen in some (see Fig. 6*D*), but not all strips (and even in strips from the same animals), in the presence of 10 μM PE (Fig. 1*B*) while a stronger rebound occurred in rabbit femoral artery in the presence of 100 μM PE as was also seen in porcine carotid artery (Etter *et al.* 2001).

SNP-induced prevention of PE-induced contraction. Pre-treatment with SNP during the resting state inhibited the initial development and suppressed the steady-state amplitude of 10 μM PE-induced contraction in denuded rabbit femoral artery smooth muscle ($n = 4$; Fig. 2). This inhibition is concentration dependent, with an EC_{50} for

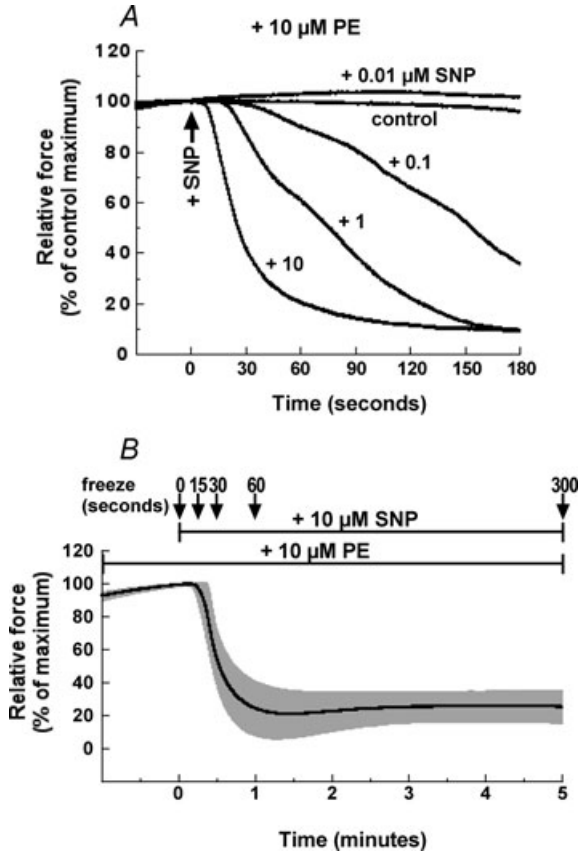

Figure 1. Concentration–response relationship of SNP-induced relaxation of PE-induced contraction in denuded rabbit femoral artery smooth muscle strips
A, representative time courses of relaxation when various concentrations of SNP are applied at the peak of contraction 3 min after 10 μM PE stimulation ($n = 4$). *B*, average ($n = 5$) time course of 10 μM SNP-induced relaxation of PE-induced contraction 3 min after PE stimulation with S.E.M. (grey). The arrows indicate the freezing time points for protein phosphorylation measurements.

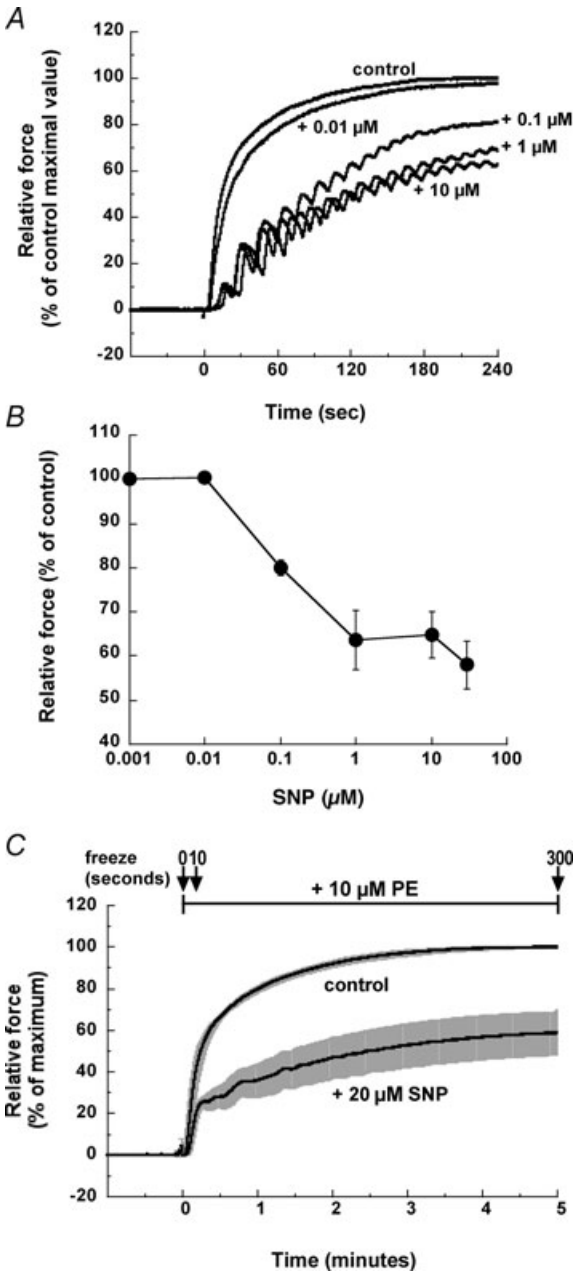

Figure 2. Time course and concentration–response relationship of SNP-induced inhibition of PE-induced contraction development in denuded rabbit femoral artery smooth muscle strips
A, representative time courses of the development of 10 μM PE-induced contraction in the presence of various SNP amounts added 5 min before PE stimulation. Force was normalized with control PE-induced contraction in the absence of SNP. *B*, concentration–response relationship of SNP-induced inhibition of the steady-state level of PE-induced contraction ($n = 4$). *C*, time courses of 10 μM PE-induced contraction with S.E.M. in the presence and absence of 20 μM SNP ($n = 5$). SNP was added at rest 5 min before PE stimulation and was present throughout the experiments. The arrows indicate the freezing points at 0, 10 and 300 s after PE addition.

SNP-induced force reduction of about 0.1 μM (Fig. 2*A* and *B*). Figure 2*C* shows the average time course of PE-induced contraction in the presence and absence of 20 μM SNP ($n = 5$). To evaluate the steady state effect of SNP, resting arteries were pretreated with 20 μM SNP for 5 min before PE stimulation and frozen at 0, 10 and 300 s after PE exposure for further analyses of protein phosphorylation.

Cytoplasmic Ca^{2+} measurements

Methods for measuring intracellular Ca^{2+} were essentially similar to that of Himpens *et al.* (1990). Briefly, conditioned arterial strips were incubated in an external solution containing 10 μM fura-2 AM, 0.5% DMSO and 0.01% Pluronic F127 (Molecular Probes) for 4 h at room temperature. After loading, strips were washed in fresh external solution. Simultaneous measurements of isometric force and fura-2 fluorescence of the strips were carried out with the Muscle Research System (SI GmbH, Heidelberg, Germany; Gth & Wojciechowski, 1986). The fluorescence intensity of fura-2 through a bandpass filter of 510 nm was collected into a photomultiplier tube for alternating excitations at 340 and 380 nm using a rotating wheel, in which the fluorescence excitation filter changed every 2 ms. The fluorescence signal for each excitation light and the ratio signal (F_{340}/F_{380}) was digitized using PowerLab/8SP (ADInstruments, Colorado Springs, CO, USA) and displayed on a computer. The F_{340}/F_{380} signal was simply used as a relative $[Ca^{2+}]_i$ signal because the dissociation constant of fura-2 for cytoplasmic Ca^{2+} differs from values obtained in a test tube (Konishi *et al.* 1988). Each end of the fura-2-loaded strip was fixed in a quartz tube with two micro-tweezers, one of which was connected to a force transducer and the other to a micromanipulator to adjust the muscle length. The solutions in the tube were maintained at 30°C. The solution exchange was done using a peristaltic pump with a 2.5 ml min^{-1} perfusion rate. The half-time for the solution exchanges was 14.8 ± 0.4 s ($n = 6$) in the muscle research system and less than 0.1 s ($n = 4$) in the bubble chamber system. Thus, the time course of Ca^{2+} signals could not be compared with that of force and MLC phosphorylation obtained in the bubble chamber system.

Measurement of MLC phosphorylation

In situ phosphorylation of MLC in muscle strips was measured using two-dimensional electrophoresis as described previously (Kitazawa *et al.* 1991; Masuo *et al.* 1994). Briefly, strips either at rest or during contraction were quickly frozen in liquid-cooled propane (−150°C) and then placed atop frozen acetone containing 10% trichloroacetic acid (TCA) and kept at –80°C overnight, after which the TCA/acetone solution was gradually warmed to room temperature. The strips were washed with acetone several times to remove TCA and then dried under vacuum. Dried strips were homogenized in a glycerol sample buffer containing 0.1% SDS, 20 mM DTT, 10% glycerol and 0.1 mg ml^{-1} BSA, and centrifuged at $15\,000 \times g$ for 15 min. The supernatants were then subjected to two-dimensional electrophoresis. The isoelectric focusing tube gel with 5% pH ampholytes 4.5/5.4 (Pharmalyte, GE Healthcare) was run overnight until a constant current was reached. Then, an appropriate portion of the gel was grafted horizontally onto the top of a SDS-polyacrylamide slab gel and the second dimensional gel was run. The proteins were transferred from the polyacrylamide gels to nitrocellulose membranes. The membranes were then extensively washed in phosphate-buffered saline overnight at room temperature. The membranes were subsequently rinsed with deionized H_2O and stained with colloidal gold (Bio-Rad). The colloidal gold-stained patterns of unphosphorylated and phosphorylated MLCs were identified according to the tropomyosin position (Bárány & Bárány, 1996) followed by scanning and analysis with image processing software (Signal Analytics Co., Vienna, VA, USA). Assuming that diphosphorylated MLC generates the same contractile effect as that of monophosphorylated MLC (Umemoto *et al.* 1989), the following equation was used: Percentage phosphorylated MLC $= 100 \times (P1 + P2)/(U + P1 + P2)$ where U is unphosphorylated, P1 is monophosphorylated, and P2 is diphosphorylated MLC.

Antibodies and Western blotting

Phosphorylation of proteins was determined by a Western blotting method with 4–20% gradient SDS polyacrylamide gels using phospho-specific antibodies as described previously (Kitazawa *et al.* 2003; Dimopoulos *et al.* 2007). Phospho[Ser695]-specific MYPT1 antibody (Wooldridge *et al.* 2004) was generously provided by Dr Timothy Haystead. Phospho[Ser188]-specific RhoA antibody was obtained from Sigma. Other phospho-specific antibodies used in this study have been described previously (Kitazawa *et al.* 2000, 2003; Dimopoulos *et al.* 2007).

Western blotting experiments were carried out in duplicate. Equal amounts of the same tissue extracts were loaded onto the same polyacrylamide gel (Jule Inc., Milford, CT, USA) and the separated proteins transferred to the same nitrocellulose membrane to avoid any fluctuation in the PAGE and transfer processes. The membrane was blocked in Tris-buffered saline containing 0.05% Tween 20 and 5% non-fat milk, then cut into two, incubated with either phospho- or pan-primary antibody and then an alkaline phosphatase-conjugated secondary antibody. The immunoblots were developed with an

alkaline phosphatase substrate solution (Promega) to visualize immunoreactive proteins. The bands of alkaline phosphatase products were digitized with a colour scanner and their intensity was analysed with image processing software (Signal Analytics Co.). We compared the intensity ratio of phosphorylated protein from one set of Western blots to the total amount of CPI-17 from the paired set of Western blots.

Figure 3 shows the specificity of anti-phospho[Ser695] and [Thr696]-MYPT1 antibodies. The MYPT1 fragment mimicking residue 658–714 was phosphorylated with recombinant ROCK (Millipore), the catalytic subunit of PKA (Sigma), and ROCK plus PKA. Unphospho-, mono- and di-phosphorylated proteins were separated in a urea-lutidine gel (Kitazawa *et al.* 1999, Eto & Brautigan, 2007) (Fig. 3*A*). The same samples were subjected to SDS-PAGE and Western blotting with anti-P-MYPT1 antibodies (Fig. 3*B*). The anti-phospho[Ser695] antibody recognized the protein phosphorylated by PKA, but not proteins in the mixture of ROCK plus PKA, suggesting that the phosphorylation at Thr696 blocks the binding of the antibody at the phospho-Ser695 site (Wooldridge *et al.* 2004). On the other hand, MYPT1 singly phosphorylated by ROCK and doubly phosphorylated by ROCK plus PKA yielded a similar staining intensity with the antibody for Thr696, suggesting that the phosphorylation of MYPT1 at Ser695 does not interfere with the binding of anti-phospho[Thr696] antibody at phospho-Thr696. The specificity of other phospho- and site-specific antibodies for phosphorylated Thr38 of CPI-17 and Thr853 of MYPT1 has been demonstrated previously (Kitazawa *et al.* 2000; Dimopoulos *et al.* 2007).

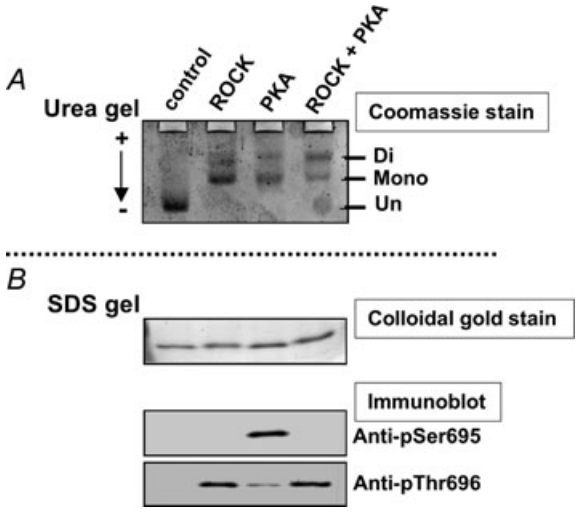

Figure 3. Specificity of anti-phospho[Ser695] and [Thr696] antibodies
A MYPT1 fragment (658–714) was phosphorylated with ROCK alone, PKA alone, or a mixture of ROCK and PKA. Twenty nanograms of phosphorylated or unphosphorylated fragments were applied onto a urea-lutidine gel (*A*; Kitazawa *et al.* 1999) to separate mono- and di-phosphorylated bands from un-phosphorylated bands. The gel was stained with Coomassie Brilliant Blue (*A*). The relative intensity of monophosphorylated band in *A* was 2, 61, 62 and 38%, and the diphosphorylated band intensity was 0, 39, 38 and 62% for control, ROCK, PKA and ROCK+PKA, respectively. The same amount of the samples was also applied onto a SDS-polyacrylamide gel (*B*) to detect total and phosphorylated amounts of fragments using, respectively, colloidal gold staining (upper panel in *B*) and Western blots with phospho- and site-specific antibodies (two lower panels). Arrow in *A* indicates the direction of current in the urea-lutidine gel. The anti-phospho[Ser695] antibody did not detect diphosphorylated fragments treated with ROCK+PKA, suggesting that this antibody recognizes only mono-phosphorylated Ser695 (Wooldridge *et al.* 2004). The anti-phospho[Thr696] antibody identified both mono- and di-phosphorylated Thr696.

Statistics

Results are expressed as the means ± S.E.M. of n experiments. Statistical significance was evaluated using ANOVA. A level of $P < 0.05$ was considered statistically significant.

Results

Ca^{2+}, force and phosphorylation during SNP-induced relaxation

To determine the molecular mechanism of SNP-induced relaxation, we examined the time course of $[Ca^{2+}]_i$, force and phosphorylation of MLC, CPI-17 (Thr38), RhoA (Ser188) and MYPT1 (Ser695, Thr696 and Thr853). Figure 4*A* illustrates a representative example of simultaneous measurement of the Fura-2 (F_{340}/F_{380}) ratio and force signals in response to 10 μM SNP during 10 μM PE-induced contraction, and indicates that $[Ca^{2+}]_i$ decreases in advance of contractile relaxation. The Ca^{2+} decrease had almost no latent period after SNP addition, in contrast to the significant latency of force reduction, which is probably due to the considerable series elastic component in smooth muscle (Halpern *et al.* 1978; Kato *et al.* 1984).

Figure 4*B* shows that, as with the change in $[Ca^{2+}]_i$, a decrease in MLC phosphorylation levels precedes the relaxation. MLC phosphorylation decreased from 47 ± 2% of total MLC at time = 0 to 33 ± 2 and 27 ± 6% (n = 4–9) at 15 and 30 s, respectively, while a relaxation did not begin until 15 s had passed. The percentile ratio of P2/P1 was not significantly different in the presence or absence of 10 μM SNP in PE-stimulated artery: 13 ± 2 (n = 30) *vs.* 7 ± 3% (n = 10), respectively. Figure 4*C* shows the time course of phosphorylation of CPI-17 at Thr38 and MYPT1 at Ser695 compared to the contractile relaxation. Similarly to MLC dephosphorylation, at 15 s CPI-17 was rapidly dephosphorylated to 58 ± 6% (n = 4) of its initial value, while MYPT1 Ser695 phosphorylation increased from negligible levels at time = 0 to 21 ± 5% at

15 s and then 56 ± 9% at 30 s ($n = 4$) with a time course similar to that seen for contractile change (Fig. 4*C*).

Neither MLC (Fig. 5*A*) nor CPI-17 (Fig. 5*B*) phosphorylation at 5 min in the presence of SNP differed significantly from their respective control, indicating a small but potentially important rebound of SNP-induced inhibition of both proteins' phosphorylation levels (Etter *et al.* 2001). A similar but smaller rebound in the average time course of contractile force can also be seen in Figs 1*B* and 6*D*. In contrast, MYPT1 Ser695 phosphorylation (Fig. 5*C*) reached near maximum at about 1 min and was maintained for up to 5 min. Dephosphorylation of MYPT1 at either Thr696 or Thr853 was not accompanied by an increase in Ser695 phosphorylation within 1 min (Fig. 5*D* and *F*). Control RhoA Ser188 phosphorylation was significantly decreased to 76 ± 5% ($n = 4$; Fig. 5*E*) at 5 min as compared to the value at 0 min while SNP prevented the decrease and maintained the Ser188 phosphorylation level at 119 ± 7% at 5 min, resulting in higher levels of Ser188 phosphorylation at 5 min in the tissue treated with SNP ($n = 3$). This relative increase in RhoA phosphorylation induced by SNP was accompanied by decreases in MYPT1 phosphorylation at Thr696 (70 ± 2% of control value, $n = 4$; Fig. 5*D*), and at Thr853 (65 ± 11% of control value, $n = 4$; Fig. 5*F*) at 5 min. Thus, the SNP-induced MLC dephosphorylation occurs initially in parallel to CPI-17 dephosphorylation, followed at steady state by slow RhoA phosphorylation at Ser188 and MYPT1 dephosphorylation at Thr696 and Thr853.

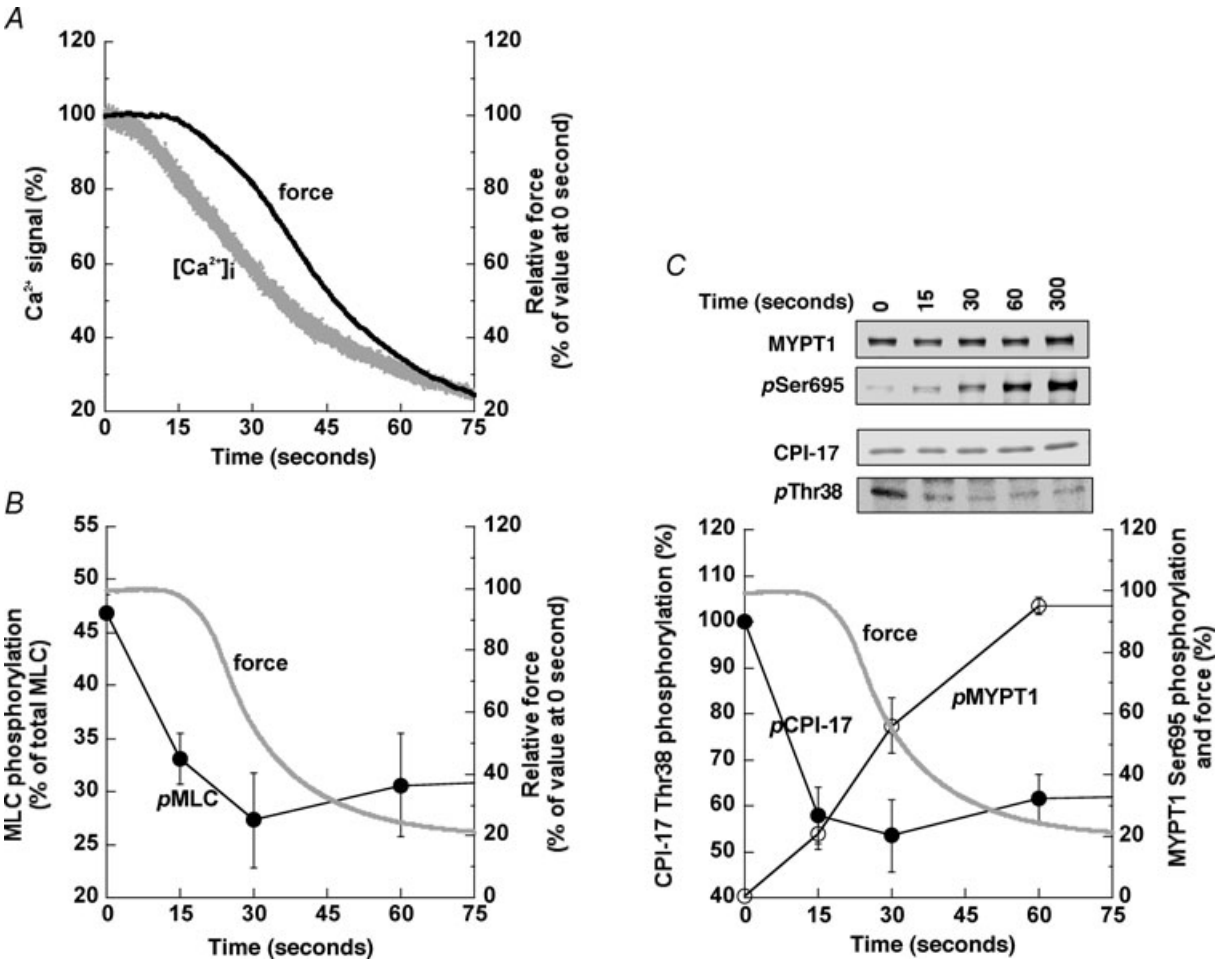

Figure 4. Time course of changes in Ca^{2+} (*A*), contractile force (*A*–*C*), and phosphorylation of MLC (*B*), CPI-17 at Thr38 (*C*) and MYPT1 at Ser695 (*C*) in response to 10 μM SNP added 3 min after PE exposure
See Fig. 1 for the protocol. *A* illustrates representative simultaneous measurements of Fura-2 (F_{340}/F_{380}) ratio signal (grey) and contractile relaxation (black). Force levels were monitored throughout the experiments (average time course of force decline in *B* and *C* is identical to that in Fig. 1*B*). Phosphorylation of MLC ($n = 4$–9, *B*), and CPI-17 and MYPT1 ($n = 4$–6, *C*) with average time course of relaxation (grey) determined using two-dimensional electrophoresis and Western blot analysis (inset in *C*), respectively. Phosphorylation values of CPI-17 at Thr38 (pCPI-17; filled circles) and MYPT1 at Ser695 (pMYPT1; open circles) were normalized with the value at 0 s and 5 min of SNP exposure, respectively.

Effects of Ca^{2+} release, Ca^{2+} influx, BK_{Ca} channel and phosphodiesterase-5 on SNP-induced relaxation

Phosphorylation of RGS-2 (Tang *et al.* 2003) or IRAG (Geiselhöringer *et al.* 2004) by PKG-1 suppresses agonist-induced Ca^{2+} release and augments Ca^{2+} uptake into the SR, and thus induces vascular smooth muscle relaxation. We examined whether depletion of SR Ca^{2+} affects the rapid relaxation and dephosphorylation of CPI-17 induced by SNP. Arterial strips were pretreated with a mixture of 1 μM ryanodine and 20 mM caffeine for 15 min to deplete the SR of Ca^{2+}. After ryanodine and caffeine were removed, PE and caffeine no longer generated a transient contraction in the absence of extracellular Ca^{2+}, indicating depletion of SR Ca^{2+}. After the ryanodine treatment, the smooth muscle strips lost the initial rapid response of contraction and CPI-17 phosphorylation in response to PE, although CPI-17 phosphorylation was gradually restored to about 60% of control and the contraction returned to a maximum level, similar for the untreated control. (Dimopoulos *et al.* 2007). As shown in Fig. 6*A*, the relaxation induced by addition of 10 μM SNP during PE-induced contraction in the presence of ryanodine was extremely delayed (Fig. 6*A*); the amplitude of the rapid component of relaxation was reduced to about half and the slow component became noticeable. Following SNP exposure, several (9 ± 1; $n = 6$) minutes were needed for the ryanodine-treated strips to relax back to the steady-state low level, as compared to 1 min for the untreated strips. The initial latent period was also prolonged to 32 ± 3 s ($n = 5$) compared to 13 ± 2 s for the paired control and the half-time of the rapid component was increased to 50 ± 3 s ($n = 4$) from 31 ± 2 s for the paired control, suggesting that the SR Ca^{2+} release and reuptake mechanism is dominant in SNP-induced rapid relaxation. Figure 6*B* shows the dephosphorylation of CPI-17 in response to SNP after ryanodine treatment. Before SNP addition, Ca^{2+} depletion suppressed CPI-17 phosphorylation to 60% of control without ryanodine. SNP induced little CPI-17 dephosphorylation in the ryanodine-treated arteries at 15 s compared to the control at time = 0, but at 30 s a small but significant dephosphorylation was observed. These results suggest that the initial rapid reduction in CPI-17

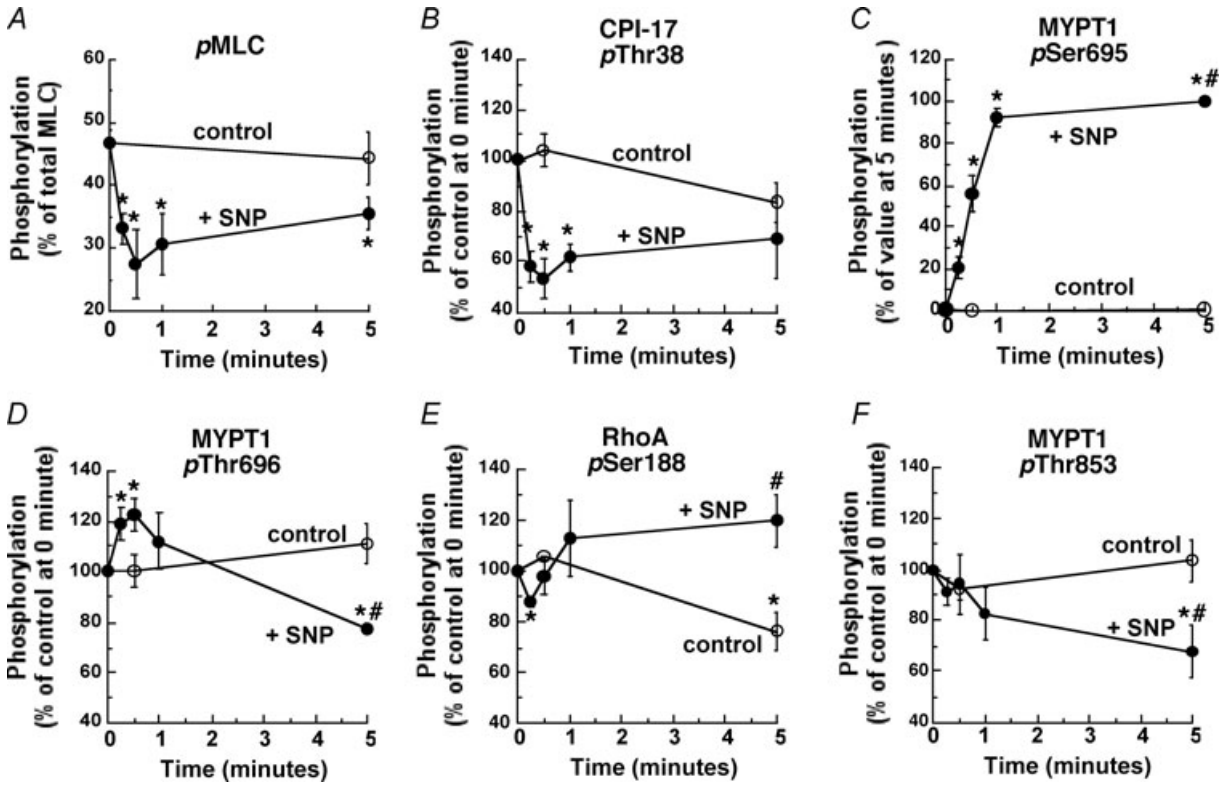

Figure 5. Time course for changes in phosphorylation of MLC (*A*, *p*MLC), CPI-17 (*B*, *p*Thr38), MYPT1 Ser695 (*C*, *p*Ser695), MYPT1 Thr696 (*D*, *p*Thr696), RhoA Ser188 (*E*, *p*Ser188) and MYPT1 Thr853 (*F*, *p*Thr853) in response to 10 μM SNP (filled circles) as compared to those of control during PE-induced contraction (open circles)

Phosphorylation values of CPI-17, RhoA and MYPT1 Thr696 and Thr853 were normalized with a respective value at 0 min while MYPT1 Ser695 phosphorylation with a value at 5 min in the presence of SNP ($n = 3$–6). Asterisks (*) show the significant difference when data points are compared to the control value at the time zero before SNP and # when data points at 5 min after SNP are compared to the control value at 5 min.

phosphorylation in response to SNP (Fig. 4*C*) depends on Ca^{2+} release/reuptake of the SR. Ryanodine treatment did not affect SNP-induced phosphorylation of Ser695 MYPT1 ($n = 4$; not shown).

BK_{Ca} channel phosphorylation by PKG-1 induces membrane hyperpolarization and a decrease in Ca^{2+} influx through inhibition of voltage-dependent Ca^{2+} channels (Alioua *et al.* 1998). We examined whether opening of the BK_{Ca} channel is involved in the rapid relaxation induced by NO using nicardipine and iberiotoxin, potent blockers of the voltage-dependent Ca^{2+} channel and BK_{Ca} channel, respectively (Nakazawa *et al.* 1988; Lovren & Triggle, 2000). Nicardipine (1 μM) partially suppressed the tonic level of PE-induced contraction prior to SNP addition, but did not inhibit the SNP-induced rapid relaxation as the half-time of 27 ± 3 s ($n = 6$) did not differ significantly from the control (Fig. 6*A*). Meanwhile, iberiotoxin (0.3 μM) slightly but significantly increased the extent of PE-induced contraction before SNP exposure and during the steady-state level of SNP-induced relaxation while having little effect on the relaxation time course (Fig. 6*C*, $n = 5$). Rather, the inhibition of BK_{Ca} channels emphasized the rebound after the rapid relaxation, resulting in an impairment of SNP-induced relaxation in the sustained phase. Taken together, these results suggest that the PKG-1/BK_{Ca} channel/Ca^{2+} channel signal is less important for the rapid phase of NO-induced relaxation, but instead aids in maintaining the relaxed state.

Phosphodiesterase-5 (PDE5; Omori & Kotera, 2007) plays a critical role in NO-induced vascular relaxation through regulation of cGMP concentration (see Murad, 2006). A specific PDE5 inhibitor, 4-[[3, 4-(methylenedioxy)benzyl]amino]-6-chloroquinazoline

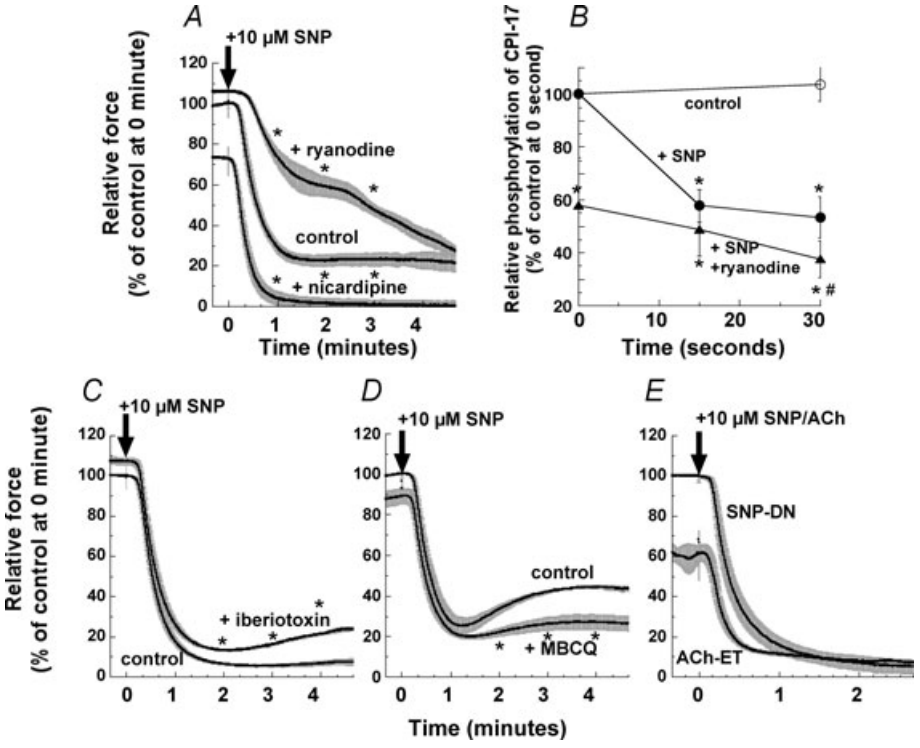

Figure 6. Effects of various inhibitors on 10 μM SNP-induced relaxation (*A*, *C* and *D*) during PE-induced contraction, and the effect of ACh on endothelium-intact compared to SNP in denuded arteries (*E*)
A, ryanodine represents the SNP-induced relaxation of ryanodine-pretreated strips with S.E.M. (see Methods) in the presence of 1 μM ryanodine ($n = 6$). Nicardipine represents the pretreatment with 1 μM nicardipine for 5 min before PE stimulation. *B*, time course of CPI-17 dephosphorylation induced by SNP in the ryanodine-treated artery compared to those of control with and without SNP in untreated artery strips, which are identical to those in Fig. 5*B*. Strips were treated with 0.3 μM iberiotoxin ($n = 5$) (*C*) and 1 μM MBCQ ($n = 4$) (*D*) for 10 min before and during PE-induced contraction. *E*, paired comparison between the time courses of SNP-induced relaxation in denuded (DN) and ACh-induced relaxation in endothelium-intact (ET) artery strips ($n = 3$ for each) from the same femoral artery. The force level developed in the endothelium-intact artery was normalized with one in the same strips thereafter treated with 100 μM L-NAME. Asterisks in the panels except *B* illustrate the significant difference at 1, 2, 3 and 4 min after SNP when the data are compared to control at the same time points. In *B*, asterisks show the significant difference when the data in the presence of SNP are compared to control at time zero in the absence of SNP, and # when the data in the ryanodine-treated artery strips after SNP are compared to the ryanodine-treated control at time zero before SNP.

(MBCQ; Salom *et al.* 2006), at 1 μM blocked the rebound in the relaxation resulting in a reduced steady-state force upon 10 μM SNP stimulation with no change in the rapid phase of relaxation ($n = 4$; Fig. 6*D*). However, the extent of the half-time and relaxation induced by low SNP concentrations (≤ 0.1 μM) was decreased by MBCQ treatment (not shown).

We examined the relaxation of arterial smooth muscle induced by endogenous NO released from the endothelium (ET). The extent of PE-induced contraction of the ET-intact femoral artery was $41 \pm 7\%$ ($n = 6$), lower than that of denuded (DN) strips (Fig. 6*E*). The suppressed contraction in the ET-intact strips was restored by pretreatment with an eNOS inhibitor, L-N^G-nitroarginine methyl ester (L-NAME; Rees *et al.* 1990) at 100 μM for 30 min, suggesting that NO is continuously generated in the ET-intact artery under control conditions (Furchgott & Vanhoutte, 1989; Neppl *et al.* 2009). Addition of 10 μM acetylcholine (ACh) to the ET-intact artery induced rapid relaxation. The latency and half-time of ACh-induced relaxation was similar to that seen for SNP-induced relaxation in DN artery (Fig. 6*E*), suggesting that SNP mimics NO production from the ET of intact vasculature. Pretreatment of endothelium-intact arteries with 100 μM L-NAME completely abolished ACh-induced relaxation (not shown).

SNP releases cyanide as a byproduct of NO production. Exogenous cyanide has an inhibitory effect on SNP-induced cGMP production and relaxation via a direct chemical reaction with SNP (Ignarro *et al.* 1986). To avoid cyanide production, another NO donor, *S*-nitroso-*N*-acetylpenicillamine (SNAP; Ferrero *et al.* 1999), which does not generate cyanide, was used to examine the relaxation of 10 μM PE-induced contraction compared to the effect of SNP. The relaxation induced by 10 μM SNAP had a half-time of 19 ± 2 s and a latent period of 11 ± 2 s ($n = 6$). Both periods were slightly shorter than those of SNP while the extent of relaxation ($25 \pm 6\%$ of control before SNAP) was similar to that of SNP ($21 \pm 6\%$, $n = 5$; Fig. 1*B*), suggesting that the rapid relaxation induced by SNP is not due to the generation of cyanide.

Effect of SNP pretreatment on contraction, Ca^{2+} and phosphorylation

Arterial smooth muscle cells *in vivo* are constantly under the influence of endothelium-derived relaxing factors consisting mainly of NO (Furchgott & Vanhoutte, 1989). To mimic these conditions, SNP (20 μM) was applied to resting denuded arterial smooth muscle prior to PE stimulation. SNP did not significantly alter the resting levels of isometric tension, $[Ca^{2+}]_i$, or phosphorylation of MLC, CPI-17 and MYPT1 Thr696 and Thr853 (Fig. 7). In contrast, SNP markedly increased resting state MYPT1 Ser695 phosphorylation to a maximal level (Fig. 7*D*), which was comparable to the phosphorylation level at 5 min in the presence of PE shown in Fig. 5*C*. The presence of SNP inhibited both the initial rising phase and the sustained phase of PE-induced contraction and $[Ca^{2+}]_i$ rise (Fig. 7*A*). The major difference in Ca^{2+} in the absence and presence of SNP was observed at the peak of the initial phase (15–20 s) and gradually reduced in the sustained phase (Fig. 7*A*). The relative force at 10 s and 5 min after PE stimulation in the presence of SNP was $9 \pm 3\%$ and $52 \pm 8\%$ ($n = 5$; Fig. 2*C*), respectively, compared to $35 \pm 1\%$ and 100% of control in the absence of SNP. Consistently, the presence of SNP significantly suppressed the increase in PE-induced MLC phosphorylation to about 50% of the control at either 10 s or 5 min (Fig. 7*B*). In the presence of SNP, CPI-17 phosphorylation was slowly induced by PE, showing a marked reduction at 10 s compared to that of 5 min (Fig. 7*C*). The phosphorylation of MYPT1 at Ser695 in the presence of SNP was much higher than the control at every time point but remained unchanged in response to PE (Fig. 7*D*). MYPT1 Thr696 phosphorylation in the presence of SNP was partially reduced to about 80% of control at either 10 s or 5 min (Fig. 7*E*). MYPT1 Thr853 phosphorylation decreased in response to SNP at 10 s and 5 min compared to control (Fig. 7*F*). Even in the presence of 20 μM SNP, however, PE still increased the phosphorylation of CPI-17 and MYPT1 Thr853 at 5 min as compared to the values at rest (Fig. 6*C* and *F*). These results suggest that NO production slows down the phosphorylation of CPI-17 and MYPT1 induced by PE, but is unable to block it completely.

Effect of SNP on phorbol ester-induced contraction and CPI-17 phosphorylation

The steady state level of CPI-17 phosphorylation is determined by reciprocal activities of kinase and phosphatase. Phorbol ester bypasses PLC activation to directly activate PKC and thus increases CPI-17 phosphorylation and contractile Ca^{2+} sensitivity in smooth muscle (Woodsome *et al.* 2001). We clamped PKC activity in the arterial strips using phorbol 12,13-dibutylate (PDBu) and asked whether CPI-17 phosphatase is activated by NO production (Fig. 8). Arteries were stimulated with 1 μM PDBu and 28 mM K^+ together for 5 min in the presence and absence of 10 μM SNP. The 28 mM K^+ solution was used to minimize the variation of PDBu-induced contraction in the resting 4 mM K^+ solution (not shown) and to monitor the effect of SNP on the basal contractility before PDBu addition. An increase in K^+ to 28 mM on its own produced $20 \pm 9\%$ ($n = 5$) of control 124 mM K^+-induced contraction (Fig. 8*A*), with negligible CPI-17

phosphorylation ($0 \pm 0\%$; $n = 4$; Fig. 8*B*). Addition of 1 μM PDBu induced contraction to $112 \pm 19\%$ of the value obtained with 124 mM K^+ at 5 min (Fig. 8*A*). PDBu markedly enhanced CPI-17 phosphorylation (Fig. 8*B* and *C*) while it had no effect on MYPT1 Thr853 phosphorylation (Fig. 8*B* and *D*). The presence of SNP reduced PDBu-induced contraction to $59 \pm 3\%$, and also 28 mM K^+ alone-induced contraction to $5 \pm 1\%$ (Fig. 8*A*). PDBu-enhanced CPI-17 phosphorylation was not reduced in response to SNP (Fig. 8*B* and *C*). On the other hand, the MYPT1 phosphorylation was significantly decreased to $49 \pm 4\%$ (Fig. 8*B* and *D*), indicating the attenuation of ROCK signals under these conditions. These results suggest that the involvement of CPI-17 phosphatase in NO signalling is minimal and the inactivation of PKC is a major cause of reduced CPI-17 phosphorylation upon NO production. Furthermore, the dephosphorylation of MYPT1 at Thr853 seems to be a cause of the reduction in NO-induced relaxation in the presence of PDBu.

Discussion

This study demonstrates that a rapid dephosphorylation of CPI-17 at Thr38, but not Ca^{2+}-independent dephosphorylation of MYPT1 at either Thr696 or Thr853, plays a crucial role in the deinhibition of MLCP in the early phase of NO-induced artery relaxation. The most critical evidence to support this hypothesis is that the decrease in CPI-17 phosphorylation in response to SNP participates in cytoplasmic Ca^{2+} reduction and MLC dephosphorylation, which are prerequisites for smooth muscle relaxation. Pre-elimination of SR Ca^{2+} release but not Ca^{2+} influx suppressed the SNP-induced rapid dephosphorylation of CPI-17 and postponed the rapid relaxation phase, suggesting that the NO-induced rapid decrease in both CPI-17 phosphorylation and contraction is significantly associated with the inhibition of Ca^{2+} release from the SR, possibly via phosphorylation of the PKG sites RGS2 (Tang *et al.* 2003) and/or IRAG (Geiselhöringer *et al.* 2004). A previous study using porcine carotid artery showed that CPI-17 is dephosphorylated in response to SNP in parallel to relaxation and elevation in $[cGMP]_i$ (Etter *et al.* 2001). However, in our study SNP-induced CPI-17 dephosphorylation achieved maximal levels within only 15 s after SNP exposure, and this rate was comparable to MLC dephosphorylation but faster than the rate of relaxation. These results are in contrast to those obtained in porcine artery, where CPI-17 dephosphorylation

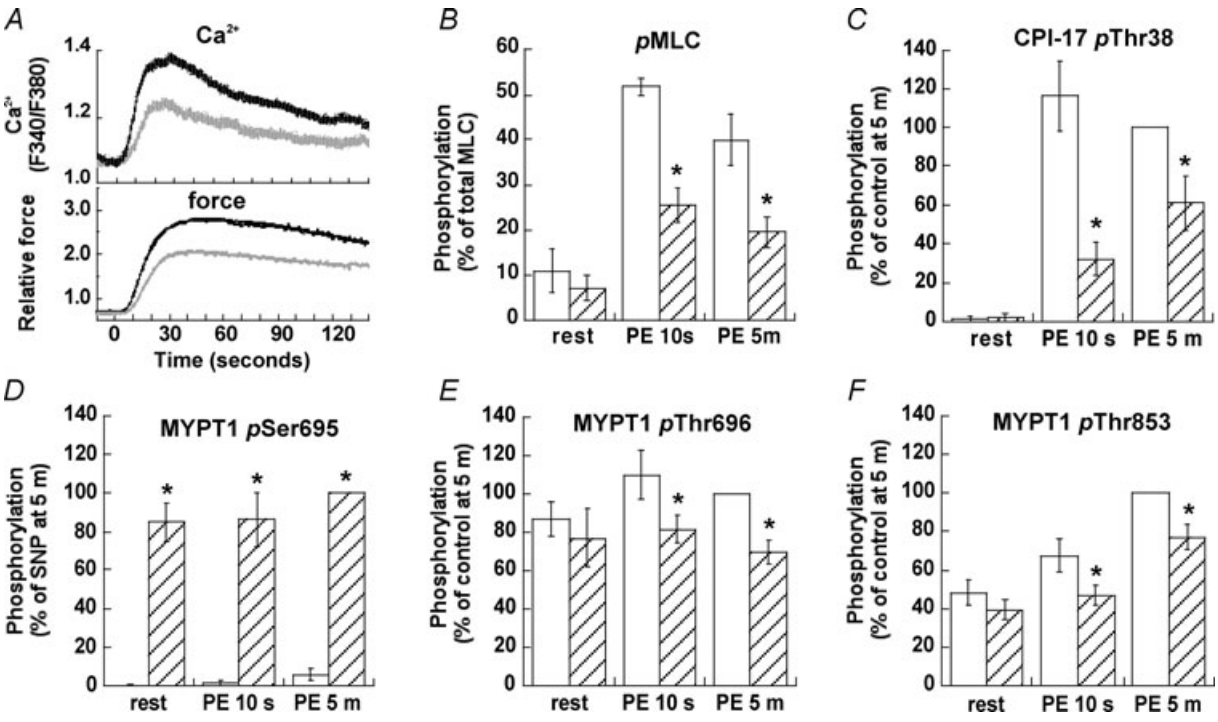

Figure 7. Effect of pretreatment with SNP on the time course of PE-induced Ca^{2+} rise (*A*, upper), force development (*A*, lower), and phosphorylation of MLC (*B*, $n = 3$), CPI-17 (*C*, $n = 6$) and MYPT1 at Ser695 (*D*, $n = 6$), Thr696 (*E*, $n = 5$) and Thr853 (*F*, $n = 6$)

Panel *A* shows a representative time course of Ca^{2+} and force in the presence (grey) and absence (black) of 20 μM SNP. Panels *B*–*F* illustrate the effect of SNP on phosphorylation of MLC, CPI-17 and MYPT1 (hatched columns) at rest and after 10 s and 5 min of PE stimulation compared to respective control values in the absence of SNP (open columns). The experimental protocol is illustrated in Fig. 2*C*. Asterisks indicate significant difference from control at the same time point.

occurred more slowly than that of MLC, and, similarly to relaxation rates, reached a minimum at 5 min of SNP exposure. SNP-induced relaxation of the strips used here was four times faster than that of porcine carotid artery (Etter *et al.* 2001). Since the thickness of the medial wall of porcine carotid artery is several times greater than that of rabbit femoral artery, the discrepancy may mainly originate from the distinct diffusion rate of SNP between the two arterial preparations.

Recently, we demonstrated the existence of at least two kinetically distinct Ca^{2+} sensitizing signal transduction pathways that lead to MLCP inhibition (Dimopoulos *et al.* 2007): a rapid phase (as rapid as the increase in $[Ca^{2+}]_i$ and MLC phosphorylation) and a slow phase (as slow as increases in contractile force). In the rapid signalling pathway, CPI-17 Thr38 phosphorylation induced by Ca^{2+}-dependent PKC is synchronously associated with Ca^{2+} release from the SR in response to PE, suggesting that a decrease in MLCP activity with increases in phosphorylated CPI-17 is kinetically coupled to an increase in Ca^{2+}-dependent MLCK activity (Isotani *et al.* 2004) that is required for a rapid development of MLC phosphorylation and smooth muscle contraction. This rapid signalling pathway appears to be interrupted by the NO–cGMP–PKG signal at multiple points. NO-induced rapid decrease in $[Ca^{2+}]_i$ proceeding to contractile relaxation is thought to be mediated by the PKG-1-induced phosphorylation of RGS2 and IRAG that inhibits the production of IP_3 and the IP_3-induced Ca^{2+} release from the SR, respectively (see Hofmann *et al.* 2006). The phosphorylated RGS2-induced suppression of PLC may also reduce DAG production. Together, NO efficiently inhibits Ca^{2+}-dependent PKC and in turn CPI-17 phosphorylation. The resulting MLCP deinhibition and MLCK deactivation decreases the activity ratio of MLCK to MLCP to induce MLC dephosphorylation and subsequent muscle relaxation. This mechanism is also expected to function for relaxation in intact vasculature because ACh also induces a relaxation in the endothelium-intact artery as rapidly as SNP does in the denuded artery. Because phospho-specific antibodies are not available, we could not confirm the rapid phosphorylation of RGS2 and/or IRAG, which deserves further investigations.

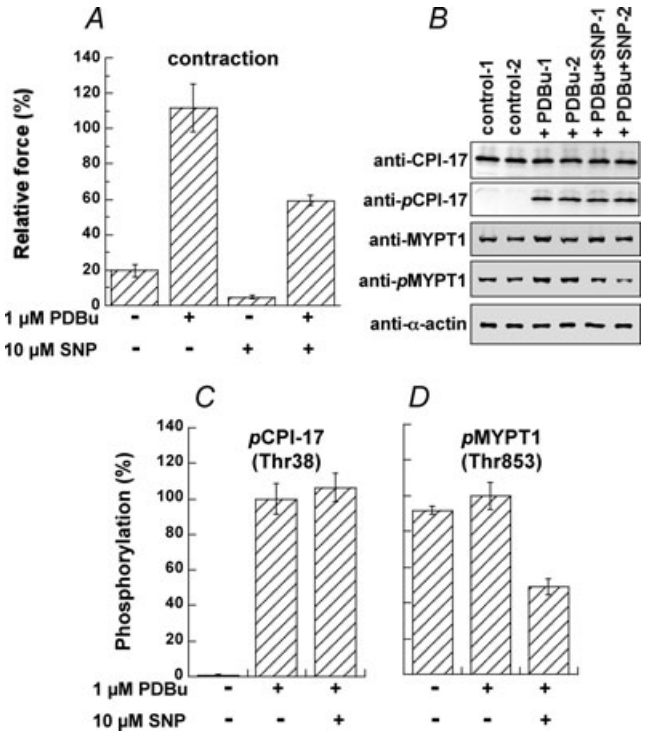

Figure 8. Effect of SNP on PDBu-induced contraction and phosphorylation of CPI-17 Thr38 and MYPT1 Thr853
Arterial strips were stimulated with 1 μM PDBu plus 28 mM K^+ for 5 min in the presence and absence of 10 μM SNP. *A*, % contraction normalized with the height of 124 mM K^+-induced contraction ($n = 4$). *B*, representative Western blots of CPI-17, pCPI-17, MYPT1, pMYPT1(Thr853) and α-actin. Twenty μg of total tissue protein was loaded in each lane except for α-actin (0.8 μg total tissue protein). *C*, relative phosphorylation of CPI-17 at Thr38 and (*D*) MYPT1 at Thr853 under various conditions. Phosphorylation values were normalized with a representative value in the artery stimulated with PDBu in the absence of SNP ($n = 4$).

The role of MYPT1 phosphorylation at Thr696 in regulating Ca^{2+} sensitivity is controversial. Three Ca^{2+}-independent signalling pathways have been identified for the slow Ca^{2+} sensitization of MLC phosphorylation during the sustained phase of agonist-induced contraction in intact artery: $G_{12/13}$/RhoA/ROCK/MYPT1(Thr853), $G_{12/13}$/RhoA/ROCK/CPI-17 and Gq/PLCβ/DAG/PKC/CPI-17 (see Dimopoulos *et al.* 2007). SNP-induced phosphorylation of PKG sites Ser695 of MYPT1 and Ser188 of RhoA did not precede the time course of MLC dephosphorylation or even relaxation. In fact, the resultant dephosphorylation of MYPT1 at either Thr696 or Thr853 was significant but occurred more slowly than the relaxation. SNP slowly augmented the phosphorylation level of RhoA Ser188 that results in reduced levels of ROCK-specific MYPT1 Thr853 phosphorylation. The extent of the reduction caused by SNP was less than that produced by the ROCK inhibitor Y-27632 at 10 μM (Dimopoulos *et al.* 2007). Therefore, NO is capable of only partial inhibition of the RhoA/ROCK signalling pathway, and the synergy achieved with the multi-point inhibition at Thr853 and Thr696 (see below) in addition to lowering of $[Ca^{2+}]_i$ is necessary to maintain the sustained phase of NO-induced relaxation. Since CPI-17 phosphorylation levels at the sustained phase of the relaxation were not significantly lower than that of the control, the importance of NO-mediated decreases in CPI-17 phosphorylation may instead diminish with time and be associated with the contractile rebound during the maintenance of NO-induced relaxation, which was also seen for porcine carotid artery (Etter *et al.* 2001).

phosphorylation of recombinant MYPT1 at Thr696 yields an inactive form of MLCP (Murányi *et al.* 2005). However, the *in situ* phosphorylation of MYPT1 Thre696 in smooth muscle tissues is rather high (∼50% of total MYPT1) at rest, and only minimally increases in response to either agonist or GTPγS, and is not significantly inhibited by Y-27632 (Kitazawa *et al.* 2003; Niiro *et al.* 2003; Wilson *et al.* 2005). Thus, MYPT1 Thr696 is unlikely to be a physiological target of the RhoA/ROCK signalling pathway, although it may be involved in pathological conditions (Seko *et al.* 2003; Guilluy *et al.* 2005; Hilgers *et al.* 2007). Wooldridge *et al.* (2004) showed in permeabilized ileum smooth muscle that PKG could directly phosphorylate MYPT1 at Ser695 and this phosphorylation blocked the adjacent Thr696 phosphorylation, suggesting a cGMP-induced prevention of phosphorylated Thr696-induced MLCP inhibition and Ca^{2+} sensitization. Recently, Nakamura *et al.* (2007) further examined the relationship between Ser695 and Thr696 under Ca^{2+}-clamped conditions in permeabilized arterial smooth muscle. They found that 8Br-cGMP stimulation increased mono-phosphorylation at Ser695 from 17 to 43% of total MYPT1 (equivalent to a relative change from 40 to 100%) and decreased mono-phosphorylation at Thr696 from 29 to 15% (equivalent to a relative change from 100 to 52%). They also revealed that 27% of MYPT1 was doubly phosphorylated at Ser695 and Thr696 and the amount of this di-phosphorylation was not altered regardless of cGMP stimulation. Thus, the total phosphorylation at Ser695, including mono- and di-phosphorylation, during either rest or PE stimulation before cGMP stimulation was already 44% of MYPT1, and the total Thr696 phosphorylation was decreased from 100 to 75% in response to 8Br-cGMP during PE stimulation (Nakamura *et al.* 2007). In contrast, using the anti-phospho[Ser695] antibody (Wooldridge *et al.* 2004) that recognizes only mono-phosphorylation at this site, Neppl *et al.* (2009) and we in this study revealed negligible amounts of Ser695 phosphorylation (e.g. less than 1% of maximum in the presence of SNP in this study) regardless of agonist stimulation before PKG stimulation in permeabilized and intact endothelium-denuded arterial smooth muscle, respectively. Considering that MYPT1 Ser695 is thought to be a PKG- and PKA-specific site (Wooldridge *et al.* 2004), 44% of Ser695 phosphorylation before PKG stimulation found by Nakamura *et al.* (2007) suggests that PKG and/or PKA are already activated in their permeabilized preparations in the absence of added cGMP. In fact, Neppl *et al.* (2009) found in endothelium-intact artery that the thromboxane A_2 (TXA_2) mimetic U-46619 increased Ser695 phosphorylation and produced a contraction in smooth muscle, indicating that U-46619 doubly stimulated endothelial TXA_2 receptors (Kent *et al.* 1993) to mediate prostacyclin release (Hunt *et al.* 1992) and thus increase cAMP in smooth muscle cells, while U-46619 also stimulates TXA_2 receptors in smooth muscle to activate G_q and $G_{12/13}$ signalling pathways to generate a contraction. It is also possible that adenine nucleotides in the experiments using permeabilized strips stimulate P2y purinergic receptors in endothelial (Furchgott & Vanhoutte, 1989) and smooth muscle cells. Our anti-phospho[Thr696] antibody that recognizes phosphorylated Thr696 regardless of Ser695 phosphorylation evidenced that NO reduced the total Thr696 phosphorylation by 30% at the steady state (5 min after SNP) of relaxation in intact artery, which is comparable to the value estimated previously (Nakamura *et al.* 2007). In our intact artery, phosphorylation of Ser695 linearly increased to more than 90% of maximum without considerable delay at 1 min after NO stimulation, while a significant decrease in Thr696 phosphorylation was not observed within 1 min, corresponding to the results of Neppl *et al.* (2009). The temporal difference in the phosphorylation between the two adjacent sites suggests that the phosphorylation of Ser695 is mainly increased only in MYPT1 without phosphorylated Thr696 and, therefore, does not accelerate the dephosphorylation of Thr696 in intact smooth muscle. Thus, the crosstalk between MYPT1 phosphorylation at Ser695 and Thr696 still remains obscure in intact smooth muscle with and without endothelium.

Protein phosphorylation levels are determined by the activity ratio of the kinase and phosphatase. CPI-17 phosphorylation reaches a maximum within 10 s in response to PE (Dimopoulos *et al.* 2007) and a minimum within 15 s in response to NO, suggesting that there are substantial amounts of CPI-17 kinase(s) and phosphatase in arterial smooth muscle. CPI-17 appears to be responsible for the rapid regulation of MLCP in response to both agonist stimulation and NO production. We proposed that inactivation of Ca^{2+}-dependent PKC resulting from NO-induced reduction in $[Ca^{2+}]_i$ and/or DAG causes a rapid CPI-17 dephosphorylation. However, the possibility that NO/cGMP/PKG signalling not only rapidly inhibits the phosphorylating kinase but also activates CPI-17 phosphatase cannot be ruled out. In fact, Bonnevier & Arner (2004) showed an ∼50% inhibition of PDBu-induced CPI-17 phosphorylation by addition of 8Br-cGMP at clamped pCa 6.0 in permeabilized intestinal smooth muscle, suggesting that cGMP activates CPI-17 phosphatase because, in the presence of a potent phosphatase inhibitor, cGMP had no effect on the PDBu-induced CPI-17 phosphorylation at clamped Ca^{2+}. In contrast, Nakamura *et al.* (2007) found no reduction of PE-induced CPI-17 phosphorylation by 8Br-cGMP at pCa 6.5 in permeabilized arterial smooth muscle, suggesting that cGMP affected neither CPI-17 kinase nor phosphatase. In this study, we showed that SNP did not reduce PDBu-enhanced CPI-17 phosphorylation in intact artery. This suggests that NO does not activate the

CPI-17 phosphatase in PDBu-stimulated intact smooth muscle, but we cannot exclude the possibility that PDBu activates PKC to a maximal level (Woodsome *et al.* 2001) that cannot be overcome by a partial activation of the phosphatase in response to NO production. The reduction of PDBu-induced contraction in response to SNP may at least partly result from a decrease in basal MYPT1 phosphorylation at Thr853, although the Thr853 phosphorylation was not enhanced in response to PDBu. Nonetheless, the CPI-17 phosphatase may be inhibited during the rebound phase (Etter *et al.* 2001). The rebounding contraction can be blocked by a PDE5 inhibitor, suggesting the feedback inhibition of guanylyl cyclase via PKG (Murthy, 2001) and the activation of PDE5 (Rybalkin *et al.* 2003). Thus, the phosphorylation of CPI-17 seems to be tightly linked to cellular cGMP levels.

In most, but not all, arterial strips used in this study, pretreatment with SNP during the resting state caused an oscillatory development of PE-induced contraction as shown in Fig. 2*A*, although the rate of rise and the steady-state amplitude of the contraction were suppressed (Fig. 2*B*). Raymond & Wendt (1996) demonstrated the synchronous oscillation of force and Ca^{2+} signals during the rebound phase of SNP-induced relaxation. A recent study of Kajioka *et al.* (2008) revealed that SNP produced oscillatory inward currents in a subpopulation (∼7%) of porcine urinary bladder smooth muscle cells. This oscillation is coupled to Ca^{2+}-activated Cl^- channel opening, indicating Ca^{2+} released from the SR ryanodine receptors. The mechanism for the SNP-induced current activation is shared with that of the oscillatory inward currents induced by agonists in the major population of the cells, where SNP does inhibit the agonist-induced oscillation. Further studies are needed to clarify the mechanism of contractile oscillation in the presence of NO and its physiological role in smooth muscle contraction.

In conclusion, we propose the hypothesis that there are two phases in the relaxation of arterial smooth muscle upon NO production. Each inhibitory phosphorylation in response to the NO/cGMP/PKG signalling has a kinetically distinct role in NO-induced relaxation in smooth muscle. NO production induces the signal to block both rapid and slow phases of agonist-induced contraction of vascular smooth muscle. The first phase includes the inhibition of Ca^{2+} release from SR that results in an inactivation of both MLCK and Ca^{2+}-dependent PKC, leading to decreased levels of phosphorylated CPI-17 and MLCP deinhibition. The later phase is sensitive to inhibitors for PDE5 and BK_{Ca}, and consists of membrane hyperpolarization directing voltage-dependent Ca^{2+} channels to close, and the dephosphorylation of MYPT1 at Thr696 and Thr853. The relative level of RhoA phosphorylation was high in the late phase, although the role of RhoA phosphorylation in MYPT1 dephosphorylation deserves further investigation. Importantly, it is now evident that phosphorylation of CPI-17 is responsible for rapid changes in MLC phosphorylation in response to both agonists and NO, whereas the phosphorylation of MYPT1 functions to control the sustained level of the contraction. We propose that the mechanism underlying the biphasic dephosphorylation of CPI-17 and MYPT1 is a key to understand the regulation of vascular smooth muscle contraction and relaxation under physiological and pathophysiological conditions.

References

Aldini G, Pirrone F, Albertini M, Orioli M, Piccoli A, Mazzola S, Clement MG & Carini M (2006). Electron spin resonance and chemiluminescence analyses to elucidate the vasodilating mechanism of sodium nitroprusside. *Mol Pharmacol* **70**, 1672–1680.

Alioua A, Tanaka Y, Wallner M, Hofmann F, Ruth P, Meera P & Toro L (1998). The large conductance, voltage-dependent, and calcium-sensitive K^+ channel, Hslo, is a target of cGMP-dependent protein kinase phosphorylation in vivo. *J Biol Chem* **273**, 32950–32956.

Bárány K & Bárány M (1996). Myosin light chain. In *Biochemistry of Smooth Muscle Contraction*, ed. Bárány M, pp. 21–35. Academic Press, San Diego.

Bonnevier J & Arner A (2004). Actions downstream of cyclic GMP/protein kinase G can reverse protein kinase C-mediated phosphorylation of CPI-17 and Ca^{2+} sensitization in smooth muscle. *J Biol Chem* **279**, 28998–29003.

Dimopoulos GJ, Semba S, Kitazawa K, Eto M & Kitazawa T (2007). Ca^{2+}-dependent rapid Ca^{2+} sensitization of contraction in arterial smooth muscle. *Circ Res* **100**, 121–129.

Eto M, Senba S, Morita F & Yazawa M (1997). Molecular cloning of a novel phosphorylation-dependent inhibitory protein of protein phosphatase-1 (CPI17) in smooth muscle: Its specific location in smooth muscle. *FEBS Lett* **410**, 356–360.

Eto M & Brautigan DL (2007). Assay for three-way interaction of protein phosphatase-1 (Glc7) with regulatory subunits plus phosphatase inhibitor-2. *Methods Mol Biol* **365**, 197–208.

Etter EF, Eto M, Wardle RL, Brautigan DL & Murphy RA (2001). Activation of myosin light chain phosphatase in intact arterial smooth muscle during nitric oxide-induced relaxation. *J Biol Chem* **276**, 34681–34685.

Feil R, Lohmann SM, de Jonge H, Walter U & Hofmann F (2003). Cyclic GMP-dependent protein kinases and the cardiovascular system: insights from genetically modified mice. *Circ Res* **93**, 907–916.

Ferrero R, Rodríguez-Pascual F, Miras-Portugal MT & Torres M (1999). Comparative effects of several nitric oxide donors on intracellular cyclic GMP levels in bovine chromaffin cells: correlation with nitric oxide production. *Br J Pharmacol* **127**, 779–787.

Fukata Y, Amano M & Kaibuchi K (2001). Rho-Rho-kinase pathway in smooth muscle contraction and cytoskeletal reorganization of non-muscle cells. *Trends Pharmacol Sci* **22**, 32–39.

Furchgott RF & Vanhoutte PM (1989). Endothelium-derived relaxing and contracting factors. *FASEB J* **3**, 2007–2018.

Ganz P, Davies PF, Leopold JA, Gimbrone MA & Alexander RW (1986). Short- and long-term interactions of endothelium and vascular smooth muscle in coculture: effects on cyclic GMP production. *Proc Natl Acad Sci U S A* **83**, 3552–3556.

Geiselhöringer A, Werner M, Sigl K, Smital P, Wörner R, Acheo L, Stieber J, Weinmeister P, Feil R, Feil S, Wegener J, Hofmann F & Schlossmann J (2004). IRAG is essential for relaxation of receptor-triggered smooth muscle contraction by cGMP kinase. *EMBO J* **23**, 4222–4231.

Guilluy C, Sauzeau V, Rolli-Derkinderen M, Guírin P, Sagan C, Pacaud P & Loirand G (2005). Inhibition of RhoA/Rho kinase pathway is involved in the beneficial effect of sildenafil on pulmonary hypertension. *Br J Pharmacol* **146**, 1010–1018.

Güth K & Wojciechowski R (1986). Perfusion cuvette for the simultaneous measurement of mechanical, optical and energetic parameters of skinned muscle fibres. *Pflugers Arch* **407**, 552–557.

Halpern W, Mulvany MJ & Warshaw DM (1978). Mechanical properties of smooth muscle cells in the walls of arterial resistance vessels. *J Physiol* **275**, 85–101.

Hartshorne DJ, Ito M & Erdodi F (2004). Role of protein phosphatase type 1 in contractile functions: myosin phosphatase. *J Biol Chem* **279**, 37211–37214.

Hilgers RH, Todd J Jr & Webb RC (2007). Increased PDZ-RhoGEF/RhoA/Rho kinase signaling in small mesenteric arteries of angiotensin II-induced hypertensive rats. *J Hypertens* **25**, 1687–1697.

Himpens B, Kitazawa T & Somlyo AP (1990). Agonist-dependent modulation of Ca^{2+}-sensitivity in rabbit pulmonary artery smooth muscle. *Pflügers Arch* **417**, 21–28.

Hofmann F, Feil R, Kleppisch T & Schlossmann J (2006). Function of cGMP-dependent protein kinases as revealed by gene deletion. *Physiol Rev* **86**, 1–23.

Huang QQ, Fisher SA & Brozovich FV (2004). Unzipping the role of myosin light chain phosphatase in smooth muscle cell relaxation. *J Biol Chem* **279**, 597–603.

Hunt JA, Merritt JE, MacDermot J & Keen M (1992). Characterization of the thromboxane receptor mediating prostacyclin release from cultured endothelial cells. *Biochem Pharmacol* **43**, 1747–1752.

Ignarro LJ, Harbison RG, Wood KS & Kadowitz PJ (1986). Dissimilarities between methylene blue and cyanide on relaxation and cyclic GMP formation in endothelium-intact intrapulmonary artery caused by nitrogen oxide-containing vasodilators and acetylcholine. *J Pharmacol Exp Ther* **236**, 30–36.

Ishizaki T, Maekawa M, Fujisawa K, Okawa K, Iwamatsu A, Fujita A, Watanabe N, Saito Y, Kakizuka A, Morii N & Narumiya S (1996). The small GTP-binding protein Rho binds to and activates a 160 kDa Ser/Thr protein kinase homologous to myotonic dystrophy kinase. *EMBO J* **15**, 1885–1893.

Isotani E, Zhi G, Lau KS, Huang J, Mizuno Y, Persechini A, Geguchadze R, Kamm KE & Stull JT (2004). Real-time evaluation of myosin light chain kinase activation in smooth muscle tissues from a transgenic calmodulin-biosensor mouse. *Proc Natl Acad Sci U S A* **101**, 6279–6284.

Kajioka S, Nakayama S, Seki N, Naito S & Brading AF (2008). Oscillatory membrane currents paradoxically induced via NO-activated pathways in detrusor cells. *Cell Calcium* **44**, 202–209.

Kato S, Osa T & Ogasawara T (1984). Kinetic model for isometric contraction in smooth muscle on the basis of myosin phosphorylation hypothesis. *Biophys J* **46**, 35–44.

Kent KC, Collins LJ, Schwerin FT, Raychowdhury MK & Ware JA (1993). Identification of functional PGH2/TxA2 receptors on human endothelial cells. *Circ Res* **72**, 958–965.

Kitazawa T, Eto M, Woodsome TP & Brautigan DL (2000). Agonists trigger G protein-mediated activation of the CPI-17 inhibitor phosphoprotein of myosin light chain phosphatase to enhance vascular smooth muscle contractility. *J Biol Chem* **275**, 9897–9900.

Kitazawa T, Eto M, Woodsome TP & Khalequzzaman M (2003). Phosphorylation of the myosin phosphatase targeting subunit and CPI-17 during Ca^{2+} sensitization in rabbit smooth muscle. *J. Physiol* **546**, 879–889.

Kitazawa T, Gaylinn BD, Denney GH & Somlyo AP (1991). G-protein-mediated Ca^{2+}-sensitization of smooth muscle contraction through myosin light chain phosphorylation. *J Biol Chem* **266**, 1708–1715.

Kitazawa T, Takizawa N, Ikebe M & Eto M (1999). Reconstitution of protein kinase C-induced contractile Ca^{2+} sensitization in Triton X-100-demembranated rabbit arterial smooth muscle. *J. Physiol* **520**, 139–152.

Kobayashi S, Kitazawa T, Somlyo AV & Somlyo AP (1989). Cytosolic heparin inhibits muscarinic and α-adrenergic Ca^{2+} release in smooth muscle. *J Biol Chem* **264**, 17997–18004.

Konishi M, Olson A, Hollingworth S & Baylor SM (1988). Myoplasmic binding of fura-2 investigated by steady-state fluorescence and absorbance measurements. *Biophys J* **54**, 1089–1104.

Lalli MJ, Shimizu S, Sutliff RL, Kranias EG & Paul RJ (1999). $[Ca^{2+}]_i$ homeostasis and cyclic nucleotide relaxation in aorta of phospholamban-deficient mice. *Am J Physiol Heart Circ Physiol* **277**, H963–970.

Lee MR, Li L & Kitazawa T (1997). Cyclic GMP causes Ca^{2+} desensitization in vascular smooth muscle by activating the myosin light chain phosphatase. *J Biol Chem* **272**, 5063–5068.

Lincoln TM, Wu X, Sellak H, Dey N & Choi CS (2006). Regulation of vascular smooth muscle cell phenotype by cyclic GMP and cyclic GMP-dependent protein kinase. *Front Biosci* **11**, 356–367.

Lovren F & Triggle C (2000). Nitric oxide and sodium nitroprusside-induced relaxation of the human umbilical artery. *Br J Pharmacol* **131**, 521–529.

Masuo M, Reardon S, Ikebe M & Kitazawa T (1994). A novel mechanism for the Ca^{2+}-sensitizing effect of protein kinase C on vascular smooth muscle: Inhibition of myosin light chain phosphatase. *J Gen Physiol* **104**, 265–286.

Matsui T, Amano M, Yamamoto T, Chihara K, Nakafuku M, Ito M, Nakano T, Okawa K, Iwamatsu A & Kaibuchi K (1996). Rho-associated kinase, a novel serine/threonine kinase, as a putative target for small GTP binding protein Rho. *EMBO J* **15**, 2208–2216.

Michael SK, Surks HK, Wang Y, Zhu Y, Blanton R, Jamnongjit M, Aronovitz M, Baur W, Ohtani K, Wilkerson MK, Bonev AD, Nelson MT, Karas RH & Mendelsohn ME (2008). High blood pressure arising from a defect in vascular function. *Proc Natl Acad Sci U S A* **105**, 6702–6707.

Morgan JP & Morgan KG (1984). Stimulus-specific patterns of intracellular calcium levels in smooth muscles of ferret portal vein. *J. Physiol* **351**, 155–167

Murad F (2006). Nitric oxide and cyclic GMP in cell signalling and drug development. *N Engl J Med* **355**, 2003–2011.

Murányi A, Derkach D, Erdodi F, Kiss A, Ito M & Hartshorne DJ (2005). Phosphorylation of Thr695 and Thr850 on the myosin phosphatase target subunit: inhibitory effects and occurrence in A7r5 cells. *FEBS Lett* **579**, 6611–6615.

Murthy KS (2001). Activation of phosphodiesterase 5 and inhibition of guanylate cyclase by cGMP-dependent protein kinase in smooth muscle. *Biochem J* **360**, 199–208.

Nakamura K, Koga Y, Sakai H, Homma K & Ikebe M (2007). cGMP-dependent relaxation of smooth muscle is coupled with the change in the phosphorylation of myosin phosphatase. *Circ Res* **101**, 712–722.

Nakazawa K, Saito H & Matsuki N (1988). Fast and slowly inactivating components of Ca-channel current and their sensitivities to nicardipine in isolated smooth muscle cells from rat vas deferens. *Pflugers Archiv* **411**, 289–295.

Neppl RL, Lubomirov LT, Momotani K, Pfitzer G, Eto M & Somlyo AV (2009). Thromboxane A2-induced bi-directional regulation of cerebral arterial tone. *J Biol Chem* **284**, 6348–6360.

Niiro N, Koga Y & Ikebe M (2003). Agonist-induced changes in the phosphorylation of the myosin binding subunit of myosin light chain phosphatase and CPI17, two regulatory factors of myosin light chain phosphatase, in smooth muscle. *Biochem J* **369**, 117–128.

Omori K & Kotera J (2007). Overview of PDEs and their regulation. *Circ Res* **100**, 309–327.

Rashatwar SS, Cornwell TL & Lincoln TM (1987). Effects of 8-bromo-cGMP on Ca^{2+} levels in vascular smooth muscle cells: possible regulation of Ca^{2+}-ATPase by cGMP-dependent protein kinase. *Proc Natl Acad Sci U S A* **84**, 5685–5689.

Raymond GL & Wendt IR (1996). Force and intracellular Ca^{2+} during cyclic nucleotide-mediated relaxation of rat anococcygeus muscle and the effects of cyclopiazonic acid. *Br J Pharmacol* **119**, 1029–1037.

Rees DD, Palmer RM, Schulz R, Hodson HF & Moncada S (1990). Characterization of three inhibitors of endothelial nitric oxide synthase in vitro and in vivo. *Br J Pharmacol* **101**, 746–752.

Rybalkin SD, Yan C, Bornfeldt KE & Beavo JA (2003). Cyclic GMP phosphodiesterases and regulation of smooth muscle function. *Circ Res* **93**, 280–291.

Salom JB, Burguete MC, Pérez-Asensio FJ, Castelló-Ruiz M, Torregrosa G & Alborch E (2006). Relaxant effect of sildenafil in the rabbit basilar artery. *Vascul Pharmacol* **44**, 10–16.

Sauzeau V, Le Jeune H, Cario-Toumaniantz C, Smolenski A, Lohmann SM, Bertoglio J, Chardin P, Pacaud P & Loirand G (2000). Cyclic GMP-dependent protein kinase signalling pathway inhibits RhoA-induced Ca^{2+} sensitization of contraction in vascular smooth muscle. *J Biol Chem* **275**, 21722–21729.

Seko T, Ito M, Kureishi Y, Okamoto R, Moriki N, Onishi K, Isaka N, Hartshorne DJ & Nakano T (2003). Activation of RhoA and inhibition of myosin phosphatase as important components in hypertension in vascular smooth muscle. *Circ Res* **92**, 411–418.

Somlyo AP & Somlyo AV (1994). Signal transduction and regulation in smooth muscle. *Nature* **372**, 231–236.

Somlyo AP & Somlyo AV (2003). Ca^{2+} sensitivity of smooth muscle and nonmuscle myosin II: Modulated by G proteins, kinases, and myosin phosphatase. *Physiol Rev* **83**, 1325–1358.

Surks HK, Mochizuki N, Kasai Y, Georgescu SP, Tang KM, Ito M, Lincoln TM & Mendelsohn ME (1999). Regulation of myosin phosphatase by a specific interaction with cGMP-dependent protein kinase 1α. *Science* **286**, 1583–1587.

Tang KM, Wang GR, Lu P, Karas RH, Aronovitz M, Heximer SP, Kaltenbronn KM, Blumer KJ, Siderovski DP, Zhu Y & Mendelsohn ME (2003). Regulator of G-protein signalling-2 mediates vascular smooth muscle relaxation and blood pressure. *Nat Med* **9**, 1506–1512.

Taylor DA & Stull JT (1988). Calcium dependence of myosin light chain phosphorylation in smooth muscle cells. *J Biol Chem* **263**, 14456–14462.

Twort CH & van Breemen C (1988). Cyclic guanosine monophosphate-enhanced sequestration of Ca^{2+} by sarcoplasmic reticulum in vascular smooth muscle. *Circ Res* **62**, 961–964.

Umemoto S, Bengur AR & Sellers JR (1989). Effect of multiple phosphorylations of smooth muscle and cytoplasmic myosins on movement in an in vitro motility assay. *J Biol Chem* **264**, 1431–1436.

Weber S, Bernhard D, Lukowski R, Weinmeister P, Wörner R, Wegener JW, Valtcheva N, Feil S, Schlossmann J, Hofmann F & Feil R (2007). Rescue of cGMP kinase I knockout mice by smooth muscle specific expression of either isozyme. *Circ Res* **101**, 1096–1103.

Wilson DP, Susnjar M, Kiss E, Sutherland C & Walsh MP (2005). Thromboxane A2-induced contraction of rat caudal arterial smooth muscle involves activation of Ca^{2+} entry and Ca^{2+} sensitization: Rho-associated kinase-mediated phosphorylation of MYPT1 at Thr-855, but not Thr-697. *Biochem J* **389**, 763–774.

Woodsome TP, Eto M, Everett A, Brautigan DL & Kitazawa T (2001). Expression of CPI-17 and myosin phosphatase correlates with Ca^{2+} sensitivity of protein kinase C-induced contraction in rabbit smooth muscle. *J Physiol* **535**, 553–564.

Wooldridge AA, MacDonald JA, Erdodi F, Ma C, Borman MA, Hartshorne DJ & Haystead TA (2004). Smooth muscle phosphatase is regulated in vivo by exclusion of phosphorylation of threonine 696 of MYPT1 by phosphorylation of Serine 695 in response to cyclic nucleotides. *J Biol Chem* **279**, 34496–34504.

Wu X, Haystead TA, Nakamoto RK, Somlyo AV & Somlyo AP (1998). Acceleration of myosin light chain dephosphorylation and relaxation of smooth muscle by telokin. Synergism with cyclic nucleotide-activated kinase. *J Biol Chem* **273**, 11362–11369.

Author contributions

T.K.: conception and design of the experimental protocol, analysis and interpretation of data, drafting and revising the manuscript, and final approval of the manuscript. S.S.: collection and analysis of data. Y-H.H.: collection and analysis of data. K.K.: collection and analysis of data. M.E.: conception and design of the experimental protocol, interpretation of data, revising and final approval of the manuscript. The experiments were performed at Boston Biomedical Research Institute at Watertown, MA, USA.

Acknowledgements

We are grateful to Dr Timothy Haystead for his phospho[Ser695]-specific MYPT1 antibody and to Dr John Gergely for his proof-reading of the manuscript. This work was supported by National Institute of Health grants R01HL070881 to T.K., and R01HL083261 and PA CURE grant to M.E.